Society For Biomaterials

A 3D *in vitro* model of the dermoepidermal junction amenable to mechanical testing

Jangwook P. Jung,[1,2,3] **Wei-Han Lin**,[1] **Megan J. Riddle**,[4] **Jakub Tolar**,[2,4,5] **Brenda M. Ogle**[1,2,5,6,7]

[1]Department of Biomedical Engineering, University of Minnesota-Twin Cities, Minneapolis, Minnesota
[2]Stem Cell Institute, University of Minnesota-Twin Cities, Minneapolis, Minnesota
[3]Department of Biological Engineering, Louisiana State University, Baton Rouge, Louisiana
[4]Department of Pediatrics, University of Minnesota-Twin Cities, Minneapolis, Minnesota
[5]Masonic Cancer Center, University of Minnesota-Twin Cities, Minneapolis, Minnesota
[6]Lillehei Heart Institute, University of Minnesota-Twin Cities, Minneapolis, Minnesota
[7]Institute for Engineering in Medicine, University of Minnesota-Twin Cities, Minneapolis, Minnesota

Received 9 April 2018; revised 20 July 2018; accepted 31 July 2018
Published online 12 September 2018 in Wiley Online Library (wileyonlinelibrary.com). DOI: 10.1002/jbm.a.36519

Abstract: Recessive dystrophic Epidermolysis Bullosa (RDEB) is caused by mutations in collagen-type VII gene critical for the dermoepidermal junction (DEJ) formation. Neither tissues of animal models nor currently available *in vitro* models are amenable to the quantitative assessment of mechanical adhesion between dermal and epidermal layers. Here, we created a 3D *in vitro* DEJ model using extracellular matrix (ECM) proteins of the DEJ anchored to a poly(ethylene glycol)-based slab (termed ECM composites) and seeded with human keratinocytes and dermal fibroblasts. Keratinocytes and fibroblasts of healthy individuals were well maintained in the ECM composite and showed the expression of collagen type VII over a 2-week period. The ECM composites with healthy keratinocytes and fibroblasts exhibited yield stress associated with the separation of the model DEJ at 0.268 ± 0.057 kPa. When we benchmarked this measure of adhesive strength with that of the model DEJ fabricated with cells of individuals with RDEB, the yield stress was significantly lower (0.153 ± 0.064 kPa) consistent with our current mechanistic understanding of RDEB. In summary, a 3D *in vitro* model DEJ was developed for quantification of mechanical adhesion between epidermal- and dermal-mimicking layers, which can be utilized for assessment of mechanical adhesion of the model DEJ applicable for Epidermolysis Bullosa-associated therapeutics. J Biomed Mater Res Part A: 106A: 3231–3238, 2018.

Key Words: Epidermolysis Bullosa, extracellular matrix, lap shear test, collagen type VII

How to cite this article: Jung JP, Lin W-H, Riddle MJ, Tolar J, Ogle BM. 2018. A 3D *in vitro* model of the dermoepidermal junction amenable to mechanical testing. J Biomed Mater Res Part A 2018:106A:3231–3238.

INTRODUCTION

In normal skin, collagen type VII (C7) interacts with dermal and epidermal proteins and forms the main component of the anchoring fibril (AF). The AF connects the layers of skin by extending from the cutaneous basement membrane and hooking into the interstitial collagen fibers of the papillary dermis.[1] Skin blistering diseases, collectively known as Epidermolysis Bullosa (EB), are characterized by tissue separation with blister formation within different layers of the skin. Of disabling forms of EB, the most severe form is recessive dystrophic EB (RDEB), which is caused by mutations in C7 gene (*COL7A1*) that encodes C7 protein.[2] Although EB is a rare heritable skin disease, there are as many as 20,000–30,000 affected individual in the USA and the worldwide estimated incidence is about half a million individuals.[3]

To better understand the etiology of EB, animal models have aided studies to understand EB initiation, progression, and the utility of new therapeutic strategies.[4] In particular, C7 null mice (*Col7a1*−/−) have been used for pilot studies of recombinant protein-based[5] or bone marrow cell-based therapies.[6] In a hypomorphic mouse model (about 10% of normal C7 level), wild-type (WT) fibroblasts were applied to resist the separation of dermoepidermal junction (DEJ) following induced stress.[7] In a canine REDB model, highly efficient transduction of epidermal autograft showed firm adhesion of DEJ over a 2-year period.[8] However, these models still lack the capacity to accurately test the mechanical integrity of the DEJ due to the thin and intercalating nature of the epidermis. Many emerging 3D engineered platforms were generated to mimic the DEJ *in vitro*,[9–12] but none were developed to assess the mechanical adhesion of the

Additional Supporting Information may be found in the online version of this article.
Correspondence to: J. P. Jung; e-mail: jjung1@lsu.edu
Contract grant sponsor: National Institutes of Health R01 HL137204 (BMO)

DEJ. In addition, other human skin equivalents primarily aim to reconstruct full-thickness skin,[9–11,13–15] not to model the DEJ components.

Here, we built a 3D *in vitro* platform to model the cells and extracellular matrix (ECM) components of the DEJ amenable to testing the resistance of the model DEJ to shear stress. The model DEJ (Fig. 1) was formed with ECM proteins to anchor keratinocytes or fibroblasts, mimicking epidermis and dermis, respectively. Intercalating basement membrane protein, namely laminin (LN)-111 was layered in between epidermal- and dermal-mimicking hydrogels to produce a trilayer composite. We hypothesized that normal, healthy keratinocytes will adhere better to the basement membrane protein than nonbasement membrane protein and that mechanical adhesion is primarily mediated by the molecular adhesion between keratinocytes and the LN-111 in the model DEJ. At various time points after generation of the composite, the model DEJ was tested for mechanical integrity as a means to evaluate disease states.

MATERIALS AND METHODS

Formation of surface-functionalized ECM composites

The PEG-NCL[16] hydrogel with 6% (wt/vol) concentration was used to mimic the epidermal layer, while 3% (wt/vol) hydrogel was used to mimic the dermal layer. The stiffness of the epidermal- and dermal-mimicking layers was around 7.9 and 0.7 kPa, respectively (Fig. 1b).

Cultures of keratinocytes and fibroblasts

Patient-derived cell lines of WT keratinocytes (WTKCs; female), RDEB patient-derived keratinocytes (pKCs; male), and dermal fibroblasts (dFBs; male) were obtained following parental consent and approval from the University of Minnesota Institutional Review Board. These cell lines were tested for karyotyping, genetic fingerprinting, and mycoplasma contamination in March 2018. The result of karyotyping was normal. Genetic fingerprinting showed that the DNA of cultured cells matched the DNA of the patients. The result of mycoplasma contamination was negative. Cell lines derived from the biopsies were frozen and banked for further experiments. To form confluent cell layers for the DEJ model, KCs at a density of 10^5 cells/cm^2 were seeded on the modified epidermal hydrogel layers, while hdFBs at a density of 5.0×10^3 cells/cm^2 were seeded on the modified dermal hydrogel layers. After 24 h of culture, LN or FN (5 μg/cm^2) was added on top of KC or hdFB layers for KC/LN/FB or KC/FN/FB groups and, then, the ECM composites were stacked together to form *in vitro* DEJ. These stacked slabs were cultured for 2 days before lap shear test.

Transepithelial electrical resistance

KCs were plated at 2.5×10^5 cells/cm^2 in cell culture inserts (cat # PICM01250; Millicell, Billerica, MA) or on the modified epidermal-mimicking layer in the inserts with the medium for normal KC culture for 24 h. After 24 h, the calcium concentration of the medium was increased from 0.06 to 1.5 mM by adding calcium chloride (cat # C1016; Sigma-

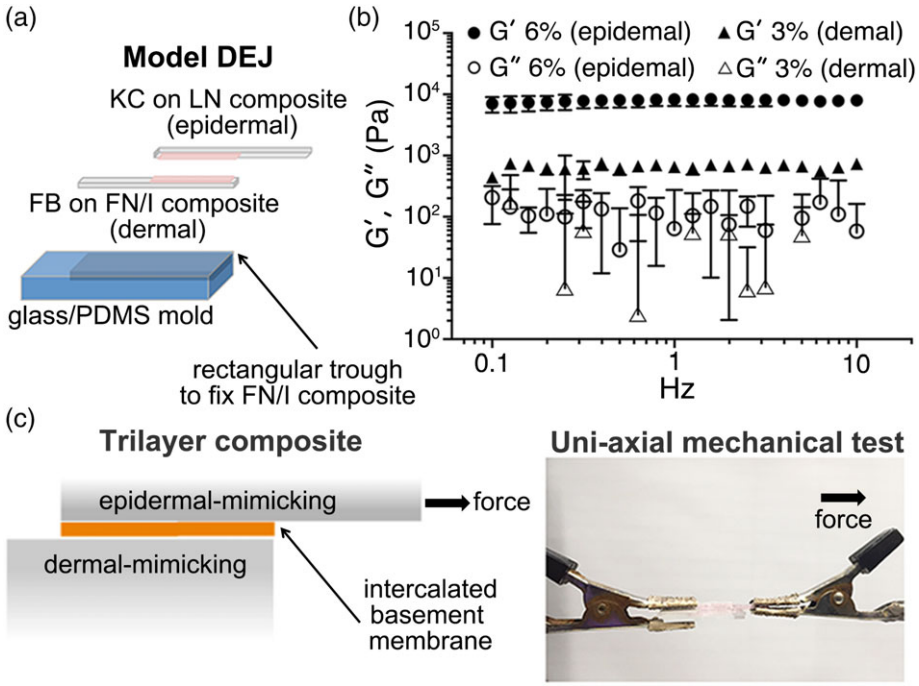

FIGURE 1. Formation of the model dermoepidermal junction utilizing ECM composites. (a) 3D trilayer composites were produced with epidermal- or dermal-mimicking ECM composites and the basement membrane protein. (b) Oscillating rheometry of the PEG-NCL hydrogel with 6% (wt/vol, epidermal mimicking) and 3% (wt/vol, dermal mimicking) concentrations. Storage (G′) and loss (G″) moduli of PEG hydrogels were determined from 0.1 to 10 Hz at 1.0% strain by frequency sweeping; mean ± SD, $n = 3$. (c) To assess the adhesion of epidermal- and dermal-mimicking ECM composites, a lap shear test via uni-axial mechanical testing was performed.

Aldrich, St. Louis, MO) to induce keratinocyte differentiation. Transepithelial electrical resistance (TEER) values were acquired everyday using an epithelial voltohmmeter (EVOM2; World Precision Instruments, Sarasota, FL). The TEER values of the inserts without cells were subtracted from each experimental value.

Immunofluroescence staining

To verify ECM-conjugation on the surface, hydrogels were stained with antifibronectin, anti-Col I, and anti-laminin-1 A and B chains' antibodies. To evaluate proteins associated at DEJ, cryosectioning was performed on the frozen blocks of stacked ECM composites.

Mechanical testing

A mesoscale lap shear test was performed with the stacked ECM composites with KC and hdFBs using a planar biaxial testing machine (Instron-Sacks Planar Biaxial Soft Tissue Testing System; Instron, Norwood, MA) equipped with a 5 N load cell. Utilizing uni-axial mechanical test (Fig. 1c), adhesion between epidermal- and dermal-mimicking layers of the model DEJ was assessed. Average shear stress (τ_{ave}) and average shear strain (γ_{ave}) were calculated as

$$\tau_{ave} = F/A_0 \quad (1)$$

$$\gamma_{ave} = \arctan(\delta/t_0) \quad (2)$$

where F is the load, A_0 is the initial contact area, δ is the displacement, and t_0 is the thickness before the lap shear test. Yield stress (σ_{yield}) was calculated as

$$\sigma_{yield} = F_{max}/A_0 \quad (3)$$

The dermal layer was fixed and kept immobile by the PDMS mold fixed onto glass, while the epidermal layer was kept immobile in the first 5 s, pulled at a crosshead speed of 18 mm/min (3% strain/s) for 35 s, and kept immobile for another 5 s. Shear stress–strain curves were obtained from force–displacement data, where yield stress was obtained from the highest value in the linear region ($R^2 > 0.99$) of the shear stress–strain curve.

Statistical analysis

One-way ANOVA with Tukey's HSD *post hoc* test for multiple comparisons was performed, where p values <0.05 were considered significant.

RESULTS

Formation of epidermal- and dermal-mimicking layers

The trilayer composites were produced via two steps. First, the surfaces of two separate PEG hydrogels were functionalized with FN, rColI and LN to produce epidermal-mimicking layers and with FN and Col I to produce dermal-mimicking layers. Second, keratinocytes and dFBs were cultured on epidermal- and dermal-mimicking surfaces, respectively (Fig. 1a).

The stiffness of respective epidermal- and dermal-mimicking layers was set to match the native stiffness of epidermis and dermis. Using large amplitude oscillatory shear deformation (strain amplitude of 10%), the dynamic shear moduli (G) of human skin decreases from 7 to 9 kPa at the superficial epidermal layer down to a stiffness of 1–2 kPa in the dermis.[17] However, using atomic force microscopy (AFM), the most probable stiffness (Young's modulus, E) of human dermis is approximately 0.77 kPa, varying from 0.1 to 10 kPa.[18] The consensus from the two studies was approximately one order of magnitude difference between epidermis and dermis. Thus, we selected 6% PEG hydrogel (7.9 kPa) for epidermal-mimicking layer and 3% PEG hydrogel (0.7 kPa) for dermal-mimicking layer (Fig. 1b). By adapting tensile loading lap shear test (ASTM F2255 Strength Properties of Tissue Adhesives in Lap Shear by Tension Loading), we established a mesoscale lap shear test platform to quantitatively assess the adhesion strength between epidermal- and dermal-mimicking layers with intercalating basement membrane proteins (Fig. 1c).

To produce surface-functionalized ECM composites, two different routes were selected (Fig. 2a). For the epidermal layer, the PEG hydrogel was functionalized with FN, rColI, and LN. The coating efficiency of FN, rColI, and LN was about 95, 91, and 83%, respectively (Fig. 2b). Using the fluorescamine assay,[19] the conjugation efficiency of Col I and FN was at least about 96 and 84%, respectively (Fig. 2c). LN conjugation to the epidermal-mimicking layer was apparent by immunofluorescence staining (Fig. 2d) and supported the attachment of WTKC and pKC (Fig. 2g,h). To generate the dermis-mimicking ECM composite, we attempted covalent conjugation of Col I or FN via NHS ester reaction chemistry to 4-armed PEG-NHS (Fig. 2a). Since a PEG-ECM composite with either PEG-Col I or PEG-FN was not sufficient to maintain hdFB monolayers for 1 day, a mixture of PEG-Col I and PEG-FN (1:1) was used to generate PEG hydrogel slabs. Immunofluorescence staining with antibodies against Col I or FN showed (Fig. 2e,f) the presentation of Col I or FN on the surface of the dermal-mimicking PEG-ECM layers. As shown in Figure 2i, hdFBs attached and maintained normal morphology on the dermal-mimicking layers.

Characterization of KCs and FBs of model DEJ

In *in vitro* cultures, epithelial cells form tight monolayers on culture inserts with porous membrane[20]; thus, we tested electrical resistance through KC monolayers using TEER measurement. As shown in Figure 3 (insert, •), the electrical resistance of WTKCs and pKCs significantly increased over 6 days in culture. The electrical resistance of WTKC significantly increased after day 3 ($11.2 \pm 2.1\ \Omega\ cm^2$) and maintained similar levels up to day 6 ($42.4 \pm 8.9\ \Omega\ cm^2$), while that of pKC increased immediately after inducing KC differentiation with high [Ca^{2+}] medium (see further detail in the "Materials and Methods" section), peaked at day 3 ($38.8 \pm 0.5\ \Omega\ cm^2$) and gradually decreased until day 6 ($12.4 \pm 6.1\ \Omega\ cm^2$). The peak electrical resistance of WTKC

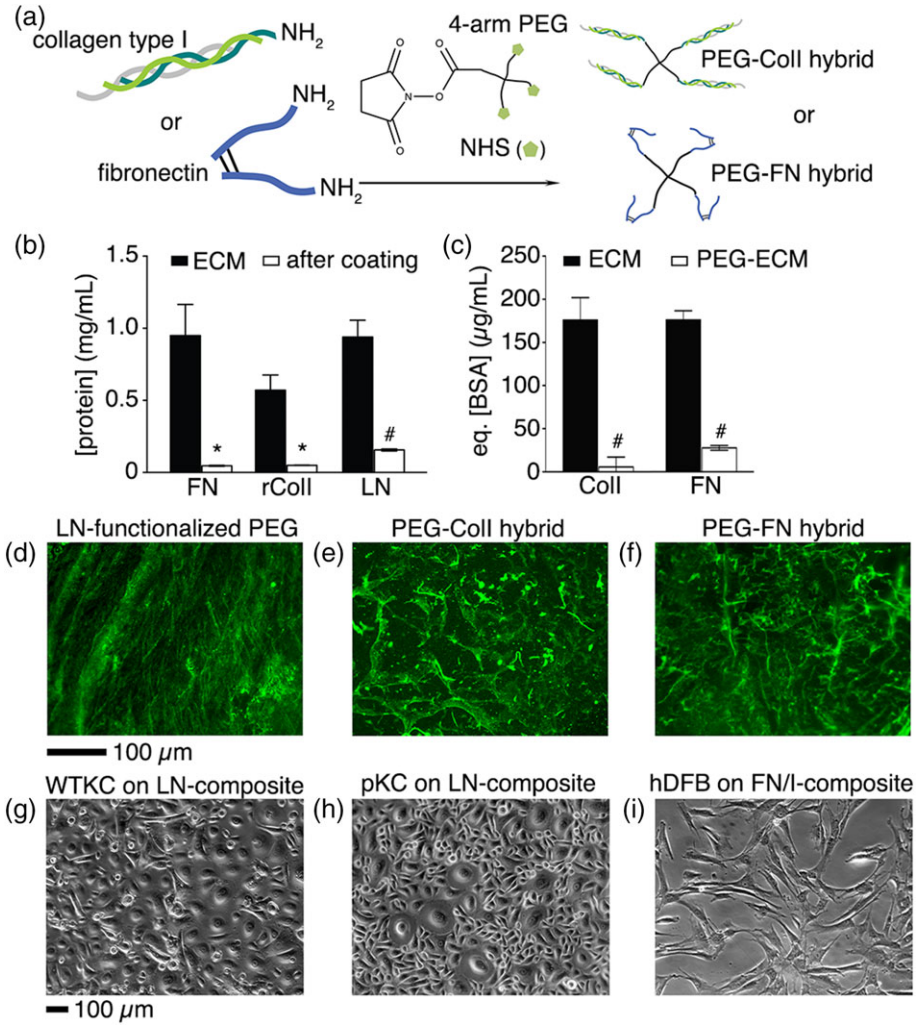

FIGURE 2. Conjugation of ECM proteins to PEG slab. (a) Conjugation of Col I and FN to NHS-functionalized 4-arm PEG. In (b), the efficiency of FN, rColI (coating matrix), and LN coatings was assessed by the BCA assay, mean ± SD, $n = 3$, Student's t-test, #$p < 0.01$ and *$p < 0.05$. In (c), the efficiency of Col I or FN conjugation to PEG was assessed by the fluorescamine assay to quantify primary amines available in Col I or FN, mean ± SD, $n = 4$, Student's t-test, #$p < 0.01$. Surface functionalized ECM composites were stained with anti-ECM antibodies to verify the distribution of LN (d), Col I (e), and FN (f). One day after culture initiation, WTKCs (g), pKCs (h), and hdFBs (i) were remained attached. Scale bars, 100 μm.

is approximately 18% higher than that of pKC at day 3, indicative of pathological nature of pKC. KCs cultured on ECM composites did not sustain electrical resistance despite generating a confluent layer (Fig. 3a,b, composite, ■). Since the ECM composites were formed in a mold and transferred to culture inserts, complete blockage of electrical current through gaps between ECM composite and insert sidewall was challenging. Due to the swelling of PEG-NCL hydrogels,[16] *in situ* formation of ECM composites in a culture insert was also unsuccessful. *In situ* formation of polypeptide or collagen type I coatings do not suffer the same issue as the thicker hydrogels (see Supporting Information Fig. S1). To gain an accurate measure of TEER of KC of the model DEJ, an alternative assay is needed, which could include, a custom-designed platform or microfluidic device.[21–23] Nevertheless, TEER confirmed the difference of forming KC integrity between WTKC and pKC.

To further assess whether epidermal- and dermal-mimicking ECM composites can form the model DEJ, we formed trilayer composites with and without ECM proteins intercalated between epidermal- and dermal-mimicking ECM composites. These trilayer composites were cryosectioned to verify the expression of proteins associated with the DEJ. As shown in Figure 4a–d, WTKCs consistently express C7 (red) and cK5 (green). In contrast, the expression of C7 from pKC was apparently none (Fig. 4e,f) and minimal from the trilayer composites with intercalated LN (Fig. 4g,h). The expression of vimentin from hdFB was present but less frequently detectable compared to C7 or cK5, owing to at least 20-fold lower seeding density of hdFBs than that of KCs.

Mesoscale lap shear test

The shear modulus of the PEG control (no ECM, no cell layers) was determined as 0.172 ± 0.017 kPa. All the other groups, either with intercalated LN (basement membrane) or with FN (nonbasement membrane) between the dermal- and epidermal-mimicking layers, showed a slight increase (all are above 0.2 kPa) compared to the PEG control. The

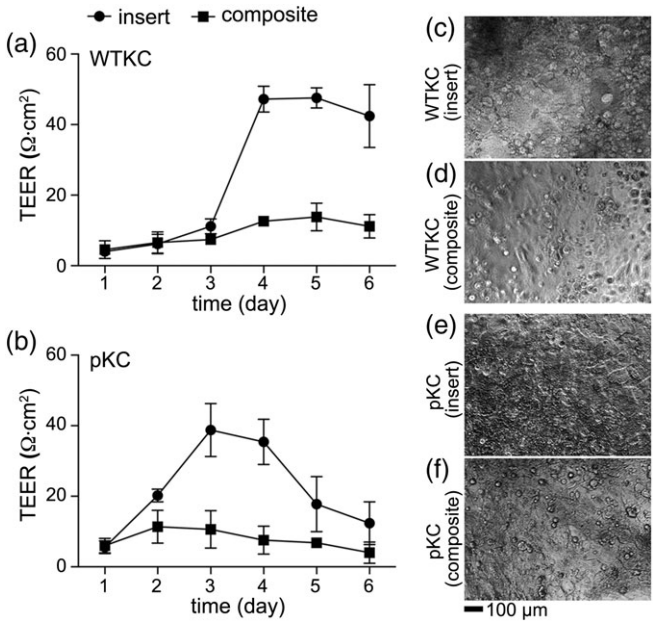

FIGURE 3. TEER measurement on tissue culture insert and on ECM composites. The electrical resistance through WTKC and pKC monolayers was measured over 6 days of culture on insert. The TEER of WTKC was significantly increased and maintained over 6 days (a) while that of pKC was peaked and diminished over 6 days, indicative of lacking the capability of forming tight monolayers of pKC, mean ± SD, $n = 3$. Morphologies of WTKC at day 5 on insert (c) and on epidermal-mimicking layer (d). Morphologies of pKC at day 3 on insert (e) and epidermal-mimicking layer (f). Scale bar, 100 μm.

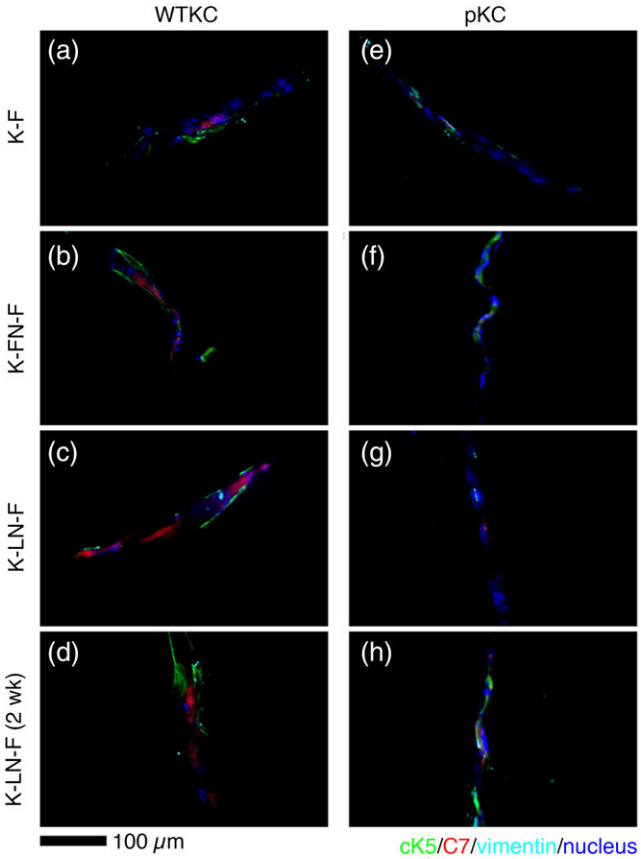

FIGURE 4. Cryosections of trilayer composites. Trilayer composites were formed with WTKCs (a–d) and pKC (e–h), where hdFBs were used as a dermal-mimicking ECM composite for both trilayer composites. Cultures of trilayer composites with WTKC (d) and pKC (e) for 2 weeks showed similar morphologies. KCs were stained with anti-cK5 (green) and anti-C7 (red) antibodies. HdFBs were stained with anti-vimentin (cyan) antibodies. Nuclei were stained with DAPI (blue). Scale bar, 100 μm.

ECM composites with WTKC showed moderately higher shear moduli than that of pKC (Fig. 5a). However, the focus of this assessment is on the mechanical adhesion between epidermal- and dermal-mimicking layers, that is, evaluating σ_{yield} or the stress at break, rather than the shear modulus of trilayer composites. The strongest adhesion was observed from the trilayer composites with WTKC and LN (Fig. 5b). The LN containing trilayer composites with WTKC showed significantly higher yield stress than that with pKC, as shown in Figure 5b. The same trend was observed in the trilayer composites with FN, though the difference was not significant between WTKC and pKC (Fig. 5b, K-LN-F vs. K-FN-F). In the absence of intercalating ECM layers, adhesion was significantly weaker than the trilayer composites with LN (Fig. 5b, K–F vs. K-LN-F). Micrographs of KC or FB monolayers were collected to verify if KCs or FBs were intact immediately before and after each mechanical test. As shown in Figure 5c–e, both KC and FB layers were still intact immediately after the lap shear test. In addition, FB layers exhibited a pattern of individual FBs parallel to the direction of uniaxial mechanical test. The mechanical adhesion of ECM composites of WTKC/FB and the adhesion of acellular ECM composites were significantly different in terms of yield stress (Fig. 5b, PEG vs. all WTKC groups, solid bars in Figure 5b), while the mechanical adhesion of pKC/FB and the adhesion of acellular ECM composites were not significantly different (PEG vs. K-F or K-FN-F; pKC open bars in Fig. 5b) or only significantly different with intercalating LN in the trilayer composite (PEG vs. K-LN-F; pKC open bar in Fig. 5b). These results indicated that the primary mechanical adhesion between the epidermal- and dermal-mimicking layers was conferred by the adhesion between KC and FB layers and mediated by the basement membrane-type proteins, not by hydrophobic adhesion between two ECM composites or non-basement membrane-type proteins, namely, FN.

DISCUSSION

Through the mesoscale lap shear platform, we begin to mimic the DEJ with layers of KCs and FBs on ECM-functionalized PEG hydrogels. It was hypothesized that WTKCs will adhere better to the basement membrane (LN) than nonbasement membrane protein (FN). As shown in Figure 5b, the results showed the statistical difference between the basement membrane trilayer composites (K-LN-F) and the nonbasement membrane trilayer composites (K-F) or between the basement membrane trilayer composite (K-LN-F) and the acellular composites (PEG). However, this difference was not statistically significant ($p = 0.083$ in

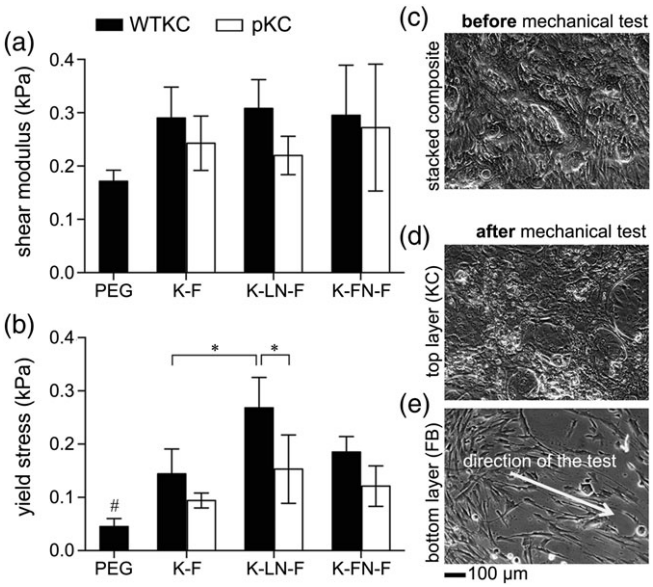

FIGURE 5. Assessment of mechanical adhesion between epidermal- and dermal-mimicking ECM composites. Shear moduli (a) and yield stresses (b) were assessed via lap shear test. Trilayer composites were maintained in culture for 2 days (c). Immediately after lap shear test, intact KCs (d) or FBs (e) on ECM composites were verified. The arrow in (e) indicates the stretched pattern of FB on the dermal-mimicking ECM composite. PEG, no ECM and cell monolayer control; K-F, trilayer composite without intercalating ECM; K-LN-F, trilayer composite with LN; K-FN-F, trilayer composite with FN, mean ± SD, $n = 3$, ANOVA Tukey–Kramer HSD *post hoc* test, $\#p < 0.01$, $*p < 0.05$.

ANOVA Tukey–Kramer *post hoc* test) when comparing the basement membrane trilayer composites (K-LN-F) to the nonbasement membrane trilayer composites (K-FN-F). Statistical differences were less discernable when shear modulus (Fig. 5a), not yield stress (Fig. 5b), was assessed. The raw data of individual stress–strain curves exhibited nonlinear shapes, while the evaluation of the shear moduli in Figure 5a was limited to the linear region ($R^2 > 0.99$) of stress–strain curves. Given the viscoelastic nature of the DEJ consisting of hydrogels, ECM proteins, and KC/FB layers, the overall nonlinear response is not surprising. However, evaluating only the elastic nature of the overall viscoelasticity may not accurately assess the mechanical adhesion conferred by the molecular association of KC/FB with LN.

While the lap shear test by tension loading (ASTM F2255 Strength Properties of Tissue Adhesives in Lap Shear by Tension Loading) is ideal to assess the strength properties of tissue adhesives, delicate biological interfaces can be easily damaged during sample preparation and loading and susceptible to distortion of the bonded interface during mechanical testing. Offsets between the grips and the specimen result in a bending moment, which artificially introduces elevated stress at the leading and tailing edges.[24] Even with proper alignment, the elastic nature of hydrogels can cause nonuniform shear stresses.[25] To overcome these shortcomings from the lap shear test, Wang and Kornfield proposed to utilize oscillating rheometry that allows quantitative determination of the yield stress of soft biological specimen with high reproducibility.[24] Using oscillating rheometry, the sample bending and distortion of adhesion between ECM proteins and embedded cells can be avoided, thus enabling more accurate measurement of the collective adhesion conferred only by the adhesion between ECM proteins and cells in the model DEJ.

To produce a more realistic model DEJ, the central component of trilayer composite, the basement membrane may include more than one ECM proteins to appropriately guide assembly of the basement membrane or more relevant ECM proteins in the native DEJ. Associated ECM proteins that are found in the basement membrane[26,27] and that are known to bind C7[28,29] includes collagen type IV, laminin-332, nidogen, and perlecan. The most recent and successful clinical trial of junctional EB (JEB; mutations in three genes, such as *LAMA3*, *LAMB3*, and *LAMC3*, encoding laminin-332) showed the critical role of laminin β3 (*LAMB3*) gene correction to regenerate the virtually entire epidermis (approximately, 0.85 m^2) of a 7-year-old patient.[30] *A priori* assumptions of ECM distribution and concentrations are hard to adjust, especially since the progression of EB varies from patient to patient. Instead, a more rigorous, systematic and efficient engineering approach to identify combinations of the basement membrane proteins would be necessary to correlate the formulation and types of the basement membrane with the developed mechanical adhesion with respect to such modulation. A rigorous, systematic calculation of basement membrane formulations[31,32] might support C7 formation to stabilize the DEJ. In addition to varying the basement membrane proteins, the other central components of trilayer composites, KCs and FBs, can be varied utilizing induced pluripotent stem cell technology,[33–35] gene editing,[36] or preconditioning of stromal cells.[37] These technologies can potentially step forward to better model the DEJ and, in the end, provide better treatment options for those with EB.

This research has the potential for broader implications. Patients suffering EB experience a stinging sensation such as being stabbed by pins or sharps even with the slightest touch. Their skin is inflamed in many places and is as fragile as a butterfly's wing, which is why pediatric patients suffering EB are often called "butterfly children." The fundamental motivation of this study of RDEB is to accurately quantify the mechanical adhesion between the dermal and epidermal layers, which could provide the molecular level mechanical interactions of basement membrane with KCs and FBs. Most skin substitutes are designed to provide either temporary impervious dressing materials or single layer skin substitutes.[38] In addition, the majority of engineered skin substitutes are developed to apply for wound healings, burns, and diabetic ulcers and only a few products were developed to treat EB such as OrCel® (Ortec International, NY) and ICX-RHY® (Intercytex, UK).[39] None of those products or platforms is suitable to investigate the micromechanical nature of the DEJ, the breakdown of the hemidesmosome within the EB skin.

Another motivation is the shortcomings of animal models, which have been utilized to advance mechanistic understanding of DEB for cell-, gene-, or protein-based therapeutics. Transgenic mice[4] or zebra fish[40]models were

suggested for suitable pre-clinical animal models. However, development of the knockout mouse as a model of the corresponding human disease is not feasible due to the absence of the corresponding gene in the mouse genome or the mutations in the mouse gene resulting in embryonic lethality.[41,42] In addition, even if animal models were readily available, the adhesion strength of the DEJ has been rarely assessed due to technical challenges of manipulating such a thin membrane. Only one recent study attempted to quantify the strength of the DEJ in a mouse model by measuring the tension from the pull-push force gauge when a sleeve of tail skin was removed.[43] The mouse model with a hypomorphic mutation in the laminin gamma 2 gene (*Lamc2*^{jeb}) developed a form of JEB, where the measured tension of B6 WT values was above 43 N and that of B6-*Lamc2*^{jeb} was below 33 N. Although this method provides a range of force required for tail skin "sleeve" removal, typical technical failures in biomechanical tests were inevitable, such as tail breakage, clamp slippage, variation of tail thickness. Thus, there is a critical need to develop a preclinical platform to quantitatively model DEB and thereby enable testing and mechanistic probing of proposed stem cell and gene-editing therapies.

In summary, a mesoscale lap shear test platform was utilized to assess the mechanical adhesion between epidermal- and dermal-mimicking layers of *in vitro* ECM composites. When both epidermal- and dermal-mimicking layers were combined to form a trilayer composite, the highest stress at break or yield stress (0.268 ± 0.057 kPa) was observed with the trilayer composite with WTKC and intercalating LN. In contrast, the yield stress of the same trilayer composite but with pKC was significantly lower (0.153 ± 0.064 kPa). The formation of tight WTKC barrier and the maintenance of C7 expression from WTKCs additionally support that this 3D *in vitro* DEJ model can be employed to quantify mechanical adhesion between epidermal and dermal layers, not only with primary cells but also possibly with gene-corrected or iPSC-derived cell types. Furthermore, modulating the composition of intercalated ECM proteins in the mode DEJ can elucidate the role of ECM proteins on the etiology of DEB.

ACKNOWLEDGMENT

The authors thank Lily Xia for the assistance in cultures of KC and FB, Cindy Eide for the verification of KC and FB cell lines, Maryn Cavalier for the preparation of PEG precursors and ECM composites, and Prof. Karl Matlin (Department of Surgery, University of Chicago) for providing MDCK cells. We also would like to acknowledge the use of Instron-Sacks Soft Tissue Testing System in the Tissue Mechanics Laboratory.

REFERENCES

1. Tolar J, Wagner JE. A biologic velcro patch. N Engl J Med 2015; 372(4):382–384.
2. Bruckner-Tuderman L, Mitsuhashi Y, Schnyder UW, Bruckner P. Anchoring fibrils and type VII collagen are absent from skin in severe recessive dystrophic Epidermolysis Bullosa. J Invest Dermatol 1989;93(1):3–9.
3. Uitto J. Rare heritable skin diseases: Targets for regenerative medicine. J Invest Dermatol 2012;132(11):2485–2488.
4. Bruckner-Tuderman L, McGrath JA, Clare Robinson E, Uitto J. Animal models of Epidermolysis Bullosa: Update 2010. J Invest Dermatol 2010;130(6):1485–1488.
5. Remington J, Wang X, Hou Y, Zhou H, Burnett J, Muirhead T, Uitto J, Keene DR, Woodley DT, Chen M. Injection of recombinant human type VII collagen corrects the disease phenotype in a murine model of dystrophic Epidermolysis Bullosa. Mol Ther 2009; 17(1):26–33.
6. Tolar J, Ishida-Yamamoto A, Riddle M, McElmurry RT, Osborn M, Xia L, Lund T, Slattery C, Uitto J, Christiano AM, Wagner JE, Blazar BR. Amelioration of epidermolysis bullosa by transfer of wild-type bone marrow cells. Blood 2009;113(5):1167–1174.
7. Fritsch A, Loeckermann S, Kern JS, Braun A, Bost MR, Bley TA, Schumann H, von Elverfeldt D, Paul D, Erlacher M, Berens von Rautenfeld D, Hausser I, Fässler R, Bruckner-Tuderman L. A hypomorphic mouse model of dystrophic Epidermolysis Bullosa reveals mechanisms of disease and response to fibroblast therapy. J Clin Invest 2008;118(5):1669–1679.
8. Gache Y, Pin D, Gagnoux-Palacios L, Carozzo C, Meneguzzi G. Correction of dog dystrophic Epidermolysis Bullosa by transplantation of genetically modified epidermal autografts. J Invest Dermatol 2011;131(10):2069–2078.
9. Benny P, Badowski C, Lane EB, Raghunath M. Making more matrix: Enhancing the deposition of dermal–epidermal junction components in vitro and accelerating organotypic skin culture development, using macromolecular crowding. Tissue Eng A 2014;21(1–2): 183–192.
10. Itoh M, Umegaki-Arao N, Guo Z, Liu L, Higgins CA, Christiano AM. Generation of 3D skin equivalents fully reconstituted from human induced pluripotent stem cells (iPSCs). PLoS One 2013;8(10):e77673.
11. Clement AL, Moutinho TJ Jr, Pins GD. Micropatterned dermal–epidermal regeneration matrices create functional niches that enhance epidermal morphogenesis. Acta Biomater 2013;9(12):9474–9484.
12. Viswanathan P, Guvendiren M, Chua W, Telerman SB, Liakath-Ali K, Burdick JA, Watt FM. Mimicking the topography of the epidermal-dermal interface with elastomer substrates. Integr Biol 2016;8(1):21–29.
13. Bellas E, Seiberg M, Garlick J, Kaplan DL. In vitro 3D full-thickness skin-equivalent tissue model using silk and collagen biomaterials. Macromol Biosci 2012;12(12):1627–1636.
14. Reijnders CMA, van Lier A, Roffel S, Kramer D, Scheper RJ, Gibbs S. Development of a full-thickness human skin equivalent in vitro model derived from TERT-immortalized keratinocytes and fibroblasts. Tissue Eng A 2015;21(17–18):2448–2459.
15. Bush KA, Pins GD. Development of microfabricated dermal epidermal regenerative matrices to evaluate the role of cellular microenvironments on epidermal morphogenesis. Tissue Eng A 2012; 18(21–22):2343–2353.
16. Jung JP, Sprangers AJ, Byce JR, Su J, Squirrell JM, Messersmith PB, Eliceiri KW, Ogle BM. ECM-incorporated hydrogels cross-linked via native chemical ligation to engineer stem cell microenvironments. Biomacromolecules 2013;14(9):3102–3111.
17. Lamers E, van Kempen THS, Baaijens FPT, Peters GWM, Oomens CWJ. Large amplitude oscillatory shear properties of human skin. J Mech Behav Biomed Mater 2013;28(Suppl. C):462–470.
18. Achterberg VF, Buscemi L, Diekmann H, Smith-Clerc J, Schwengler H, Meister J-J, Wenck H, Gallinat S, Hinz B. The nano-scale mechanical properties of the extracellular matrix regulate dermal fibroblast function. J Invest Dermatol 2014;134(7): 1862–1872.
19. Udenfriend S, Stein S, Bohlen P, Dairman W, Leimgruber W, Weigele M. Fluorescamine: A reagent for assay of amino acids, peptides, proteins, and primary amines in the picomole range. Science 1972;178(4063):871–872.
20. Petrova A, Celli A, Jacquet L, Dafou D, Crumrine D, Hupe M, Arno M, Hobbs C, Cvoro A, Karagiannis P, Devito L, Sun R, Adame LC, Vaughan R, McGrath JA, Mauro TM, Ilic D. 3D in-vitro model of a functional epidermal permeability barrier from human embryonic stem cells and induced pluripotent stem cells. Stem Cell Rep 2014; 2(5):675–689.
21. Harrington H, Cato P, Salazar F, Wilkinson M, Knox A, Haycock JW, Rose F, Aylott JW, Ghaemmaghami AM. Immunocompetent 3D model of human upper airway for disease modeling and in vitro drug evaluation. Mol Pharm 2014;11(7):2082–2091.

22. Nalayanda DD, Puleo C, Fulton WB, Sharpe LM, Wang T-H, Abdullah F. An open-access microfluidic model for lung-specific functional studies at an air–liquid interface. Biomed Microdevices 2009;11(5):1081–1089.
23. Ramadan Q, Ting FCW. In vitro micro-physiological immune-competent model of the human skin. Lab Chip 2016; 16(10):1899–1908.
24. Wang M, Kornfield JA. Measuring shear strength of soft-tissue adhesives. J Biomed Mater Res B: Appl Biomater 2012;100B(3): 618–623.
25. Sitterle VB, Sun W, Levenston ME. A modified lap test to more accurately estimate interfacial shear strength for bonded tissues. J Biomech 2008;41(15):3260–3264.
26. Tolar J, Blazar BR, Wagner JE. Concise review: Transplantation of human hematopoietic cells for extracellular matrix protein deficiency in Epidermolysis Bullosa. Stem Cells 2011;29(6):900–906.
27. Chen M, Costa FK, Lindvay CR, Han Y-P, Woodley DT. The recombinant expression of full-length type VII collagen and characterization of molecular mechanisms underlying dystrophic Epidermolysis Bullosa. J Biol Chem 2002;277(3):2118–2124.
28. Woodley DT, O'Keefe EJ, McDonald JA, Reese MJ, Briggaman RA, Gammon WR. Specific affinity between fibronectin and the Epidermolysis Bullosa acquisita antigen. J Clin Invest 1987;79(6): 1826–1830.
29. Behrens DT, Villone D, Koch M, Brunner G, Sorokin L, Robenek H, Bruckner-Tuderman L, Bruckner P, Hansen U. The epidermal basement membrane is a composite of separate laminin- or collagen IV-containing networks connected by aggregated perlecan, but not by nidogens. J Biol Chem 2012;287(22):18700–18709.
30. Hirsch T, Rothoeft T, Teig N, Bauer JW, Pellegrini G, De Rosa L, Scaglione D, Reichelt J, Klausegger A, Kneisz D, Romano O, Secone Seconetti A, Contin R, Enzo E, Jurman I, Carulli S, Jacobsen F, Luecke T, Lehnhardt M, Fischer M, Kueckelhaus M, Quaglino D, Morgante M, Bicciato S, Bondanza S, De Luca M. Regeneration of the entire human epidermis using transgenic stem cells. Nature 2017;551:327.
31. Jung JP, Hu D, Domian IJ, Ogle BM. An integrated statistical model for enhanced murine cardiomyocyte differentiation via optimized engagement of 3D extracellular matrices. Sci Rep 2015;5:18705.
32. Jung JP, Moyano JV, Collier JH. Multifactorial optimization of endothelial cell growth using modular synthetic extracellular matrices. Integr Biol 2011;3(3):185–196.
33. Sebastiano V, Zhen HH, Haddad B, Bashkirova E, Melo SP, Wang P, Leung TL, Siprashvili Z, Tichy A, Li J, Ameen M, Hawkins J, Lee S, Li L, Schwertschkow A, Bauer G, Lisowski L, Kay MA, Kim SK, Lane AT, Wernig M, Oro AE. Human COL7A1-corrected induced pluripotent stem cells for the treatment of recessive dystrophic Epidermolysis Bullosa. Sc Transl Med 2014;6(264):264ra163.
34. Tolar J, McGrath JA, Xia L, Riddle MJ, Lees CJ, Eide C, Keene DR, Liu L, Osborn MJ, Lund TC, Blazar BR, Wagner JE. Patient-specific naturally gene-reverted induced pluripotent stem cells in recessive dystrophic Epidermolysis Bullosa. J Invest Dermatol 2014;134(5): 1246–1254.
35. Tolar J, Xia L, Riddle MJ, Lees CJ, Eide CR, McElmurry RT, Titeux M, Osborn MJ, Lund TC, Hovnanian A, Wagner JE, Blazar BR. Induced pluripotent stem cells from individuals with recessive dystrophic Epidermolysis Bullosa. J Invest Dermatol 2011;131(4): 848–856.
36. Webber BR, Osborn MJ, McElroy AN, Twaroski K, C-l L, DeFeo AP, Xia L, Eide C, Lees CJ, McElmurry RT, Riddle MJ, Kim CJ, Patel DD, Blazar BR, Tolar J. CRISPR/Cas9-based genetic correction for recessive dystrophic Epidermolysis Bullosa. NPJ Regen Med 2016;1: 16014.
37. Perdoni C, McGrath JA, Tolar J. Preconditioning of mesenchymal stem cells for improved transplantation efficacy in recessive dystrophic Epidermolysis Bullosa. Stem Cell Res Therapy 2014;5(6):121.
38. Halim AS, Khoo TL, Yussof SJM. Biologic and synthetic skin substitutes: An overview. Indian J Plast Surg 2010;43(Suppl): S23–S28.
39. Vijayavenkataraman S, Lu WF, Fuh JYH. 3D bioprinting of skin: A state-of-the-art review on modelling, materials, and processes. Biofabrication 2016;8(3):032001.
40. Li Q, Frank M, Thisse CI, Thisse BV, Uitto J. Zebrafish: A model system to study heritable skin diseases. J Invest Dermatol 2011;131(3): 565–571.
41. Li CF, MacDonald JR, Wei RY, Ray J, Lau K, Kandel C, Koffman R, Bell S, Scherer SW, Alman BA. Human sterile alpha motif domain 9, a novel gene identified as down-regulated in aggressive fibromatosis, is absent in the mouse. BMC Genomics 2007;8(1):1–17.
42. Sercu S, Poumay Y, Herphelin F, Liekens J, Beek L, Zwijsen A, Wessagowit V, Huylebroeck D, McGrath JA, Merregaert J. Functional redundancy of extracellular matrix protein 1 in epidermal differentiation. Br J Dermatol 2007;157(4):771–775.
43. Sproule TJ, Roopenian DC, Sundberg JP. A direct method to determine the strength of the dermal–epidermal junction in a mouse model for Epidermolysis Bullosa. Exp Dermatol 2012; 21(6):453–455.